

UNDERSTANDING HIGH-INDEX SADDLE DYNAMICS VIA NUMERICAL ANALYSIS*

LEI ZHANG[†], PINGWEN ZHANG[‡], AND XIANGCHENG ZHENG[§]

Abstract. High-index saddle dynamics (HiSD) serves as a competitive instrument in searching the any-index saddle points and constructing the solution landscape of complex systems. The Lagrangian multiplier terms in HiSD ensure the Stiefel manifold constraint, which, however, are dropped in the commonly-used discrete HiSD scheme and are replaced by an additional Gram-Schmidt orthonormalization. Though this scheme has been successfully applied in various fields, it is still unclear why the above modification does not affect its effectiveness. We recover the same form as HiSD from this scheme, which not only leads to error estimates naturally, but indicates that the mechanism of Stiefel manifold preservation by Lagrangian multiplier terms in HiSD is nearly a Gram-Schmidt process (such that the above modification is appropriate). The developed methods are further extended to analyze the more complicated constrained HiSD on high-dimensional sphere, which reveals more mechanisms of the constrained HiSD in preserving several manifold properties.

Keywords. saddle point; saddle dynamics; solution landscape; error estimate; manifold property

AMS subject classifications. 37N30; 37M21

1. Introduction Searching saddle points on a complicated energy landscape is a hot but challenging topic in computational physical and chemistry [5, 12, 19, 21, 24, 31]. The saddle points can be classified by the (Morse) index, which, according to the Morse theory [20], are characterized by the maximal dimension of a subspace on which the Hessian is negative definite. There exist extensive searching algorithms for saddle points [4, 6–10, 15–18, 22, 29, 32]. This work focuses on a high-index saddle dynamics (HiSD) approach [27] for finding an index- k saddle point of the energy functional $E(x)$ and constructing solution landscapes [13, 25, 26, 28]

$$\begin{cases} \frac{dx}{dt} = \mathcal{S}(t), \\ \frac{dv_i}{dt} = \mathcal{R}_i(t) + \mathcal{L}_i(t), \quad 1 \leq i \leq k, \end{cases} \quad (1.1)$$

where

$$\begin{cases} \mathcal{S}(t) := \beta \left(I - 2 \sum_{j=1}^k v_j v_j^\top \right) F(x), \\ \mathcal{R}_i(t) := \gamma J(x) v_i, \\ \mathcal{L}_i(t) := \gamma \left(-v_i v_i^\top - 2 \sum_{j=1}^{i-1} v_j v_j^\top \right) J(x) v_i. \end{cases} \quad (1.2)$$

Here $x \in \mathbb{R}^d$ represents the state variable, $v_i (i = 1, \dots, k)$ are k directional variables constructing the unstable subspace of the target saddle point, $F(x) = -\nabla E(x)$, $J(x) =$

*Received date, and accepted date (The correct dates will be entered by the editor).

[†]Beijing International Center for Mathematical Research, Center for Machine Learning Research, Center for Quantitative Biology, Peking University, Beijing, 100871, China (zhangl@math.pku.edu.cn)

[‡]School of Mathematics and Statistics, Wuhan University, Wuhan, 430072, China; School of Mathematical Sciences, Laboratory of Mathematics and Applied Mathematics, Peking University, Beijing, 100871, China (pzhang@pku.edu.cn)

[§]School of Mathematics, Shandong University, Jinan, 250100, China (xzhang@sdu.edu.cn)

$-\nabla^2 E(x)$, and $\beta, \gamma > 0$ are relaxation parameters. It is shown in [27] that a linearly stable steady state of (1.1) is an index- k saddle point. From the original derivations of HiSD in [27], the $\mathcal{R}_i(t)$ arises from minimizing the Rayleigh quotient, while $\mathcal{L}_i(t)$ is introduced via the Lagrangian multiplier method to ensure the Stiefel manifold constraint, that is, the orthonormality of directional vectors $\{v_i(t)\}_{i=1}^k$ for any $t > 0$, provided that the initial values $\{v_i(0)\}_{i=1}^k$ are orthonormal.

1.1. Motivation An efficient algorithm for HiSD is developed in [26] with numerical solutions $\{x_n\}_{n=1}^N$ and $\{v_{i,n}\}_{i=1,n=1}^{k,N}$

$$\begin{cases} x_n = x_{n-1} + \tau \mathcal{S}^{n-1}, \\ \tilde{v}_{i,n} = v_{i,n-1} + \tau \mathcal{R}_i^{n-1}, \quad 1 \leq i \leq k, \\ v_{i,n} = \text{GramSchmidt}(v_{1,n}, \dots, v_{i-1,n}; \tilde{v}_{i,n}), \quad 1 \leq i \leq k, \end{cases} \quad (1.3)$$

equipped with the initial state x_0 and orthonormal initial directional vectors $\{v_{i,0}\}_{i=1}^k$, where

$$\begin{aligned} \mathcal{S}^{n-1} &:= \beta \left(I - 2 \sum_{j=1}^k v_{j,n-1} v_{j,n-1}^\top \right) F(x_{n-1}), \\ \mathcal{R}_i^{n-1} &:= \gamma J(x_{n-1}) v_{i,n-1}. \end{aligned} \quad (1.4)$$

We observe that the Lagrangian multiplier terms in \mathcal{L}_i in HiSD are dropped in this scheme and the Gram-Schmidt orthonormalization is thus critical to enforce the Stiefel manifold constraint.

A related work [33] analyzes the algorithm (1.3) with the second scheme replaced by

$$\begin{aligned} \tilde{v}_{i,n} &= v_{i,n-1} + \tau \mathcal{R}_i^{n-1} + \tau \mathcal{L}_i^{n-1} \quad \text{where} \\ \mathcal{L}_i^{n-1} &:= \gamma \left(-v_{i,n-1} v_{i,n-1}^\top - 2 \sum_{j=1}^{i-1} v_{j,n-1} v_{j,n-1}^\top \right) J(x_{n-1}) v_{i,n-1}, \end{aligned} \quad (1.5)$$

which leads to the scheme proposed in the original work [27]. In comparison with (1.3), the Lagrangian multiplier terms in \mathcal{L}_i in HiSD are reserved such that (1.5) is the exact discretization of the equation of v_i in (1.1) and the Gram-Schmidt orthonormalization serves as a perturbation that retracts the dynamics of directional vectors to the Stiefel manifold. For this reason, a perturbation analysis is carried out in [33] to perform error estimates, which ensures that the numerical scheme evolves along the dynamical pathway of continuous HiSD such that the numerical scheme also converges to the same target saddle point of HiSD. Other numerical treatments such as the projection methods for differential equations on manifolds [11], which project the dynamics of directional vectors back to the Stiefel manifold at each time step, could also be applied with error estimates derived from the conclusions in [11].

However, numerical analysis for the scheme (1.3) could not follow the aforementioned ones since the discrete dynamics of directional vectors is not consistent with its continuous analogues. Due to the loss of Lagrangian multiplier terms in (1.3), the Gram-Schmidt orthonormalization in (1.3) is no longer a perturbation or projection but may impose a substantial adjustment to enforce the Stiefel manifold constraint as the Lagrangian multiplier terms do in the continuous HiSD. In order to understand the

effectiveness of the scheme shown in [26] and ensure its convergence to the same target saddle point as continuous HiSD, it is natural to investigate whether these modifications in numerical discretization change the mechanisms of HiSD in preserving manifold properties and to what extent deviate the numerical solutions from the latent trajectory of HiSD.

1.2. Contribution The main contributions of this work are enumerated to address the aforementioned issues:

- (i) We prove that the dynamics of directional vectors in (1.1) could be recovered from the superposition of the discrete dynamics of minimizing the Rayleigh quotient and the Gram-Schmidt orthonormalization, i.e. the second and the third equations in (1.3), respectively, with the error of order $O(\tau)$ (cf. Theorem 2.1). Several novel splittings such as (2.12) and the subsequent estimates of (2.15) are proposed to explore the hidden structures of the Gram-Schmidt process and to gradually get over the nonlinearity and coupling. This result not only reduces the error estimate of (1.3) to that for standard system of differential equations, but reveals that the mechanism of Stiefel manifold preservation in HiSD is close to the Gram-Schmidt process, which improves the understanding of HiSD via numerical analysis.
- (ii) We extend the results for the constrained HiSD on the unit sphere S^{d-1} [23,30], which has been successfully applied in computing constrained saddle points of, e.g. the Bose-Einstein condensation [2,3]

$$\begin{cases} \frac{dx}{dt} = \mathcal{S}(t) - xx^\top F(x), \\ \frac{dv_i}{dt} = \mathcal{R}_i(t) + \mathcal{L}_i(t) - xx^\top J(x)v_i + xv_i^\top F(x), \quad 1 \leq i \leq k, \end{cases} \quad (1.6)$$

where \mathcal{S} , \mathcal{R}_i and \mathcal{L}_i are defined as before with relaxation parameters $\beta = \gamma = 1$ for simplicity. Specifically, (a) we prove that the dynamics of the state variable in (1.6) could be recovered from the superposition of the discrete unconstrained discrete gradient dynamics (i.e. the first scheme of (1.3)) and the retraction via the vector normalization, while (b) the dynamics of directional vectors could be recovered from the superposition of the discrete dynamics of minimizing the Rayleigh quotient, the vector transport and the Gram-Schmidt orthonormalization, with the error of order $O(\tau)$ (cf. Theorem 4.1). Similar to (i), these results could significantly simplify the error estimate of (1.3) and, more importantly, reveal that the mechanisms of the constrained HiSD on preserving several manifold properties (4.2) are close to the simple operations such as the vector normalization, the vector transport and the Gram-Schmidt orthonormalization.

2. Recovery of HiSD The main purpose of this section is to prove that the dynamics of directional vectors could be recovered by combining the second and the third equations in the scheme (1.3), except for high-order perturbations. This result not only demonstrates the statements in (i), but will facilitate error estimates in subsequent sections.

We make the assumptions following [33,34]:

Assumption A: There exists a constant $L > 0$ such that the following linearly growth

and Lipschitz conditions hold under the standard l^2 norm $\|\cdot\|$ of a vector or a matrix

$$\begin{aligned} \|J(x_2) - J(x_1)\| + \|F(x_2) - F(x_1)\| &\leq L\|x_2 - x_1\|, \\ \|F(x)\| &\leq L(1 + \|x\|), \quad x, x_1, x_2 \in \mathbb{R}^d. \end{aligned}$$

It is shown in [33] that, under the Assumption A, $\|x_n\|$ is bounded by some fixed constant for $1 \leq n \leq N$, which, based on the scheme of $\tilde{v}_{i,n}$ in (1.3), implies the boundedness of $\|\tilde{v}_{i,n}\|$. Furthermore, according to the formula of the Gram-Schmidt procedure, the third equation of (1.3) could be written in a clearer manner

$$v_{i,n} = \frac{1}{Y_{i,n}} \left(\tilde{v}_{i,n} - \sum_{j=1}^{i-1} (\tilde{v}_{i,n}^\top v_{j,n}) v_{j,n} \right) \quad (2.1)$$

where

$$Y_{i,n} := \left\| \tilde{v}_{i,n} - \sum_{j=1}^{i-1} (\tilde{v}_{i,n}^\top v_{j,n}) v_{j,n} \right\| = \left(\|\tilde{v}_{i,n}\|^2 - \sum_{j=1}^{i-1} (\tilde{v}_{i,n}^\top v_{j,n})^2 \right)^{1/2}. \quad (2.2)$$

This explicit formula will be frequently used as the third equation of (1.3) in the following derivations.

We first prove a preliminary estimate for the difference $v_{i,n} - v_{i,n-1}$ for future use. Throughout the paper we use Q to denote a generic positive constant that may assume difficult values at different occurrences.

LEMMA 2.1. *For τ small enough the following estimate holds for $1 \leq i \leq k$ and $1 \leq n \leq N$*

$$\|v_{i,n} - v_{i,n-1}\| \leq Q\tau. \quad (2.3)$$

Here Q is independent from i , τ and N .

Proof. We first prove the conclusion for $i=1$. From the second and the third equations of (1.3) with $i=1$ we obtain

$$\begin{aligned} v_{1,n} &= \frac{\tilde{v}_{1,n}}{\|\tilde{v}_{1,n}\|} = \tilde{v}_{1,n} + \frac{\tilde{v}_{1,n}}{\|\tilde{v}_{1,n}\|} (1 - \|\tilde{v}_{1,n}\|) \\ &= v_{1,n-1} + \tau\gamma J(x_{n-1})v_{1,n-1} + \frac{\tilde{v}_{1,n}}{\|\tilde{v}_{1,n}\|} (1 - \|\tilde{v}_{1,n}\|), \end{aligned}$$

which implies

$$\|v_{1,n} - v_{1,n-1}\| \leq Q\tau + |1 - \|\tilde{v}_{1,n}\||.$$

We incorporate this with

$$\|\tilde{v}_{1,n}\| = \|v_{1,n-1} + \tau\gamma J(x_{n-1})v_{1,n-1}\| = 1 + O(\tau)$$

to get $\|v_{i,n} - v_{i,n-1}\| \leq Q_1\tau$ for some positive constant Q_1 . Then we assume that

$$\|v_{j,n} - v_{j,n-1}\| \leq Q_j\tau \quad (2.4)$$

for $1 \leq j \leq i-1$ for some $1 \leq i \leq k$ and for some positive constants Q_1, \dots, Q_{i-1} . We intend to prove that

$$\|v_{i,n} - v_{i,n-1}\| \leq Q_i\tau$$

for some positive constant Q_i . Here Q_i could be greater than Q_1, \dots, Q_{i-1} . We invoke the second equation of (1.3) in the third equation of (1.3) to obtain

$$v_{i,n} = \frac{1}{Y_{i,n}} \left(v_{i,n-1} + \tau\gamma J(x_{n-1})v_{i,n-1} - \sum_{j=1}^{i-1} (v_{i,n-1}^\top v_{j,n})v_{j,n} - \tau\gamma \sum_{j=1}^{i-1} (v_{i,n-1}^\top J(x_{n-1})^\top v_{j,n})v_{j,n} \right). \quad (2.5)$$

We apply $v_{i,n-1}^\top v_{j,n-1} = 0$ to obtain

$$v_{i,n} - v_{i,n-1} = \frac{1}{Y_{i,n}} \left(v_{i,n-1}(1 - Y_{i,n}) + \tau\gamma J(x_{n-1})v_{i,n-1} - \sum_{j=1}^{i-1} (v_{i,n-1}^\top (v_{j,n} - v_{j,n-1}))v_{j,n} - \tau\gamma \sum_{j=1}^{i-1} (v_{i,n-1}^\top J(x_{n-1})^\top v_{j,n})v_{j,n} \right), \quad (2.6)$$

which leads to

$$\|v_{i,n} - v_{i,n-1}\| \leq \frac{1}{Y_{i,n}} \left(|1 - Y_{i,n}| + \sum_{j=1}^{i-1} \|v_{j,n} - v_{j,n-1}\| + Q\tau \right). \quad (2.7)$$

As for τ small enough

$$\begin{aligned} Y_{i,n} &= \left(\|\tilde{v}_{i,n}\|^2 - \sum_{j=1}^{i-1} (\tilde{v}_{i,n}^\top v_{j,n})^2 \right)^{1/2} \\ &= \left(\|v_{i,n-1} + \tau\gamma J(x_{n-1})v_{i,n-1}\|^2 - \sum_{j=1}^{i-1} ((v_{i,n-1} + \tau\gamma J(x_{n-1})v_{i,n-1})^\top v_{j,n})^2 \right)^{1/2} \\ &= \left(1 + 2\tau\gamma v_{i,n-1}^\top J(x_{n-1})v_{i,n-1} + O(\tau^2) - \sum_{j=1}^{i-1} (v_{i,n-1}^\top (v_{j,n} - v_{j,n-1}) + \tau\gamma v_{i,n-1}^\top J(x_{n-1})^\top v_{j,n})^2 \right)^{1/2} \\ &\in \left[1 \pm Q \left(\sum_{j=1}^{i-1} \|v_{j,n} - v_{j,n-1}\|^2 + \tau \right) \right]^{1/2}, \end{aligned} \quad (2.8)$$

we obtain

$$|1 - Y_{i,n}| \leq |1 - Y_{i,n}^2| \leq Q \left(\sum_{j=1}^{i-1} \|v_{j,n} - v_{j,n-1}\|^2 + \tau \right). \quad (2.9)$$

We incorporate this estimate with (2.7) to obtain

$$\|v_{i,n} - v_{i,n-1}\| \leq \frac{Q \sum_{j=1}^{i-1} \|v_{j,n} - v_{j,n-1}\|^2 + \sum_{j=1}^{i-1} \|v_{j,n} - v_{j,n-1}\| + Q\tau}{\left(1 - Q \left(\sum_{j=1}^{i-1} \|v_{j,n} - v_{j,n-1}\|^2 + \tau \right) \right)^{1/2}}, \quad (2.10)$$

which, together with the hypothesis (2.4), leads to

$$\|v_{i,n} - v_{i,n-1}\| \leq \frac{Q\tau^2 + Q\tau}{(1 - Q(\tau^2 + \tau))^{1/2}} \leq Q_i\tau.$$

Thus we obtain (2.4) for $j = i$, which completes the induction procedure. Then we select Q in (2.3) as $\max\{Q_1, \dots, Q_k\}$ to complete the proof. \square

We then prove the main theorem of this section.

THEOREM 2.1. *For τ small enough, combining the second and the third equations in (1.3), which correspond to the discrete dynamics of minimizing the Rayleigh quotient and the Gram-Schmidt procedure, respectively, leads to the discrete dynamics of directional vectors in (1.1) for $1 \leq n \leq N$ and $1 \leq i \leq k$*

$$\frac{v_{i,n} - v_{i,n-1}}{\tau} = \mathcal{R}_i^{n-1} + \mathcal{L}_i^{n-1} + O(\tau). \quad (2.11)$$

REMARK 2.1. *From this theorem we observe that the Lagrangian multiplier terms are recovered in the second equation of (1.3) by invoking the third equation of (1.3) such that, except for the error $O(\tau)$, (2.11) is exactly the explicit numerical scheme of the equation of v_i in (1.1). As τ tends to 0, (2.11) and thus the superposition of the second and the third equations in (1.3) converges to the dynamics of directional vectors in HiSD, which may indicate that the Gram-Schmidt process has the same effects as the Lagrangian multiplier terms that justifies the claims in (i).*

Furthermore, in error estimates we could easily generate the error equations by subtracting the reference equation of v_i from (2.11). In other words, (2.11) provides a much more feasible form to generate the error equations than the original scheme (i.e. the second and the third equations in (1.3)).

Proof. From the last-but-one equality of (2.8) and Lemma 2.1, we have

$$Y_{i,n} = (1 + 2\tau\gamma v_{i,n-1}^\top J(x_{n-1})v_{i,n-1} + O(\tau^2))^{1/2}.$$

Then we introduce a novel splitting

$$\begin{aligned} \frac{1}{Y_{i,n}} &= 1 + \frac{1 - Y_{i,n}^2}{Y_{i,n}(1 + Y_{i,n})} \\ &= 1 + \frac{-2\tau\gamma v_{i,n-1}^\top J(x_{n-1})v_{i,n-1} + O(\tau^2)}{Y_{i,n}(1 + Y_{i,n})} \\ &= 1 - \tau\gamma v_{i,n-1}^\top J(x_{n-1})v_{i,n-1} \\ &\quad - 2\tau\gamma v_{i,n-1}^\top J(x_{n-1})v_{i,n-1} \left(\frac{1}{Y_{i,n}(1 + Y_{i,n})} - \frac{1}{2} \right) \\ &\quad + \frac{O(\tau^2)}{Y_{i,n}(1 + Y_{i,n})}. \end{aligned} \quad (2.12)$$

By (2.9) and Lemma 2.1, the (\dots) term in the last-but-one right-hand side term of (2.12) could be estimated as

$$\left| \frac{1}{Y_{i,n}(1 + Y_{i,n})} - \frac{1}{2} \right| = \frac{|1 - Y_{i,n}|}{1 + Y_{i,n}} \left(\frac{1}{Y_{i,n}} + \frac{1}{2} \right) \leq Q|1 - Y_{i,n}| \leq Q\tau. \quad (2.13)$$

Thus the last-but-one right-hand side term of (2.12) is indeed an $O(\tau^2)$ term, and we invoke this in (2.12) to obtain

$$\frac{1}{Y_{i,n}} = 1 - \tau\gamma v_{i,n-1}^\top J(x_{n-1})v_{i,n-1} + O(\tau^2). \quad (2.14)$$

We substitute $1/Y_{i,n}$ in (2.5) by this equation to obtain

$$\begin{aligned}
v_{i,n} &= (1 - \tau\gamma v_{i,n-1}^\top J(x_{n-1}) v_{i,n-1} + O(\tau^2)) \\
&\quad \times \left(v_{i,n-1} + \tau\gamma J(x_{n-1}) v_{i,n-1} - \sum_{j=1}^{i-1} (v_{i,n-1}^\top v_{j,n}) v_{j,n} \right. \\
&\quad \quad \left. - \tau\gamma \sum_{j=1}^{i-1} (v_{i,n-1}^\top J(x_{n-1})^\top v_{j,n}) v_{j,n} \right) \\
&= v_{i,n-1} + \tau\gamma J(x_{n-1}) v_{i,n-1} - \sum_{j=1}^{i-1} (v_{i,n-1}^\top v_{j,n}) v_{j,n} \\
&\quad - \tau\gamma \sum_{j=1}^{i-1} (v_{i,n-1}^\top J(x_{n-1})^\top v_{j,n}) v_{j,n} \\
&\quad - \tau\gamma v_{i,n-1}^\top J(x_{n-1}) v_{i,n-1} v_{i,n-1} \\
&\quad + \tau\gamma \sum_{j=1}^{i-1} (v_{i,n-1}^\top v_{j,n}) v_{i,n-1}^\top J(x_{n-1}) v_{i,n-1} v_{j,n} + O(\tau^2) \\
&=: \sum_{m=1}^6 A_m + O(\tau^2).
\end{aligned} \tag{2.15}$$

From the definition of $\tilde{v}_{j,n}$ for $1 \leq j \leq i-1$, we have

$$v_{i,n-1}^\top \tilde{v}_{j,n} = v_{i,n-1}^\top (v_{j,n-1} + \tau\gamma J(x_{n-1}) v_{j,n-1}) = \tau\gamma v_{i,n-1}^\top J(x_{n-1}) v_{j,n-1}. \tag{2.16}$$

We apply this to rewrite A_3 as

$$\begin{aligned}
A_3 &= - \sum_{j=1}^{i-1} (v_{i,n-1}^\top v_{j,n}) v_{j,n} \\
&= - \sum_{j=1}^{i-1} v_{i,n-1}^\top (v_{j,n} - \tilde{v}_{j,n}) v_{j,n} - \sum_{j=1}^{i-1} v_{i,n-1}^\top \tilde{v}_{j,n} v_{j,n} \\
&= - \sum_{j=1}^{i-1} v_{i,n-1}^\top (v_{j,n} - \tilde{v}_{j,n}) v_{j,n} - \tau\gamma \sum_{j=1}^{i-1} v_{i,n-1}^\top J(x_{n-1}) v_{j,n-1} v_{j,n} \\
&=: A_{3,1} + A_{3,2}.
\end{aligned}$$

By Lemma 2.1, $A_{3,2}$ could be reformulated as

$$\begin{aligned}
A_{3,2} &= -\tau\gamma \sum_{j=1}^{i-1} v_{i,n-1}^\top J(x_{n-1}) v_{j,n-1} v_{j,n-1} \\
&\quad + \tau\gamma \sum_{j=1}^{i-1} v_{i,n-1}^\top J(x_{n-1}) v_{j,n-1} (v_{j,n-1} - v_{j,n}) \\
&= -\tau\gamma \sum_{j=1}^{i-1} v_{i,n-1}^\top J(x_{n-1}) v_{j,n-1} v_{j,n-1} + O(\tau^2).
\end{aligned} \tag{2.17}$$

To estimate $A_{3,1}$, from the third equation of (1.3), we have

$$v_{j,n} - \tilde{v}_{j,n} = \left(\frac{1}{Y_{j,n}} - 1 \right) \tilde{v}_{j,n} - \frac{1}{Y_{j,n}} \sum_{l=1}^{j-1} (\tilde{v}_{j,n}^\top v_{l,n}) v_{l,n}, \tag{2.18}$$

which implies

$$v_{i,n-1}^\top (v_{j,n} - \tilde{v}_{j,n}) = \left(\frac{1}{Y_{j,n}} - 1 \right) v_{i,n-1}^\top \tilde{v}_{j,n} - \frac{1}{Y_{j,n}} \sum_{l=1}^{j-1} \tilde{v}_{j,n}^\top v_{l,n} v_{i,n-1}^\top v_{l,n}. \quad (2.19)$$

From (2.14) and (2.16), the first right-hand side term of (2.19) is an $O(\tau^2)$ term, while the second right-hand side term could be reformulated as

$$\begin{aligned} & -\frac{1}{Y_{j,n}} \sum_{l=1}^{j-1} \tilde{v}_{j,n}^\top v_{l,n} v_{i,n-1}^\top v_{l,n} \\ &= -\frac{1}{Y_{j,n}} \sum_{l=1}^{j-1} \tilde{v}_{j,n}^\top (v_{l,n} - v_{l,n-1}) v_{i,n-1}^\top v_{l,n} \\ & \quad -\frac{1}{Y_{j,n}} \sum_{l=1}^{j-1} \tilde{v}_{j,n}^\top v_{l,n-1} v_{i,n-1}^\top v_{l,n}. \end{aligned} \quad (2.20)$$

By Lemma 2.1, $v_{i,n-1}^\top v_{l,n} = v_{i,n-1}^\top (v_{l,n} - v_{l,n-1})$ is an $O(\tau)$ term, and

$$\tilde{v}_{j,n}^\top v_{l,n-1} = v_{l,n-1}^\top (v_{j,n-1} + \tau\gamma J(x_{n-1})v_{j,n-1}) = \tau\gamma v_{l,n-1}^\top J(x_{n-1})v_{j,n-1}$$

is also an $O(\tau)$ term. Thus, (2.20) is an $O(\tau^2)$ term, which implies (2.19) is also an $O(\tau^2)$ term. Consequently, $A_{3,1}$ is an $O(\tau^2)$ term, which, together with (2.17), leads to

$$A_3 = -\tau\gamma \sum_{j=1}^{i-1} v_{i,n-1}^\top J(x_{n-1})v_{j,n-1}v_{j,n-1} + O(\tau^2). \quad (2.21)$$

We then split A_4 as

$$\begin{aligned} A_4 &= -\tau\gamma \sum_{j=1}^{i-1} (v_{i,n-1}^\top J(x_{n-1}))^\top v_{j,n-1}v_{j,n-1} \\ & \quad -\tau\gamma \sum_{j=1}^{i-1} (v_{i,n-1}^\top J(x_{n-1}))^\top (v_{j,n} - v_{j,n-1})v_{j,n-1} \\ & \quad -\tau\gamma \sum_{j=1}^{i-1} (v_{i,n-1}^\top J(x_{n-1}))^\top v_{j,n}(v_{j,n} - v_{j,n-1}). \end{aligned}$$

By Lemma 2.1 we obtain

$$A_4 = -\tau\gamma \sum_{j=1}^{i-1} (v_{i,n-1}^\top J(x_{n-1}))^\top v_{j,n-1}v_{j,n-1} + O(\tau^2). \quad (2.22)$$

By the symmetry of J , we incorporate (2.21) and (2.22) to find that

$$\begin{aligned} A_1 + \cdots + A_5 &= v_{i,n-1} + \tau\gamma J(x_{n-1})v_{i,n-1} \\ & \quad -\tau\gamma v_{i,n-1}^\top J(x_{n-1})v_{i,n-1}v_{i,n-1} \\ & \quad -2\tau\gamma \sum_{j=1}^{i-1} (v_{i,n-1}^\top J(x_{n-1}))^\top v_{j,n-1}v_{j,n-1} + O(\tau^2). \end{aligned}$$

Therefore, in order to get (2.11), we need to show that $A_6 = O(\tau^2)$. As

$$\begin{aligned} A_6 &= \tau\gamma \sum_{j=1}^{i-1} (v_{i,n-1}^\top v_{j,n}) v_{i,n-1}^\top J(x_{n-1}) v_{i,n-1} v_{j,n} \\ &= \tau\gamma \sum_{j=1}^{i-1} v_{i,n-1}^\top (v_{j,n} - v_{j,n-1}) v_{i,n-1}^\top J(x_{n-1}) v_{i,n-1} v_{j,n}, \end{aligned}$$

we apply Lemma 2.1 again to find that A_6 is an $O(\tau^2)$ term, which completes the proof. \square

3. Error estimates and numerical experiments Based on Theorem 2.1, we prove error estimates for the numerical scheme (1.3) and perform numerical experiments to substantiate the theoretical findings.

3.1. Error estimates The error equation of e_n^x could be generated by subtracting the first equation of (1.3) from the reference equation of $x(t)$, which is obtained by discretizing the first equation of (1.1) via the Euler discretization

$$x(t_n) = x(t_{n-1}) + \tau\mathcal{S}(t_{n-1}) + O(\tau^2).$$

The error equation of $e_n^{v_i}$ could be derived by subtracting (2.11) from the reference equation of $v_i(t)$

$$v_i(t_n) = v_i(t_{n-1}) + \tau\mathcal{R}_i(t_{n-1}) + \tau\mathcal{L}_i(t_{n-1}) + O(\tau^2).$$

Based on these error equations, the error estimates could be performed following those for standard system of differential equations [1], and we thus directly state the result in the following theorem.

THEOREM 3.1. *Under the Assumption A, the following estimate holds for the scheme (1.3) for τ sufficiently small*

$$\|x(t_n) - x_n\| + \sum_{i=1}^k \|v_i(t_n) - v_{i,n}\| \leq Q\tau, \quad 1 \leq n \leq N. \quad (3.1)$$

Here Q is independent from τ , n and N .

REMARK 3.1. *Let $\{X_n\}_{n=1}^N$ and $\{V_{i,n}\}_{i=1,n=1}^{k,N}$ be numerical solutions of the scheme (1.3) with the second equation replaced by (1.5), i.e. the numerical discretization scheme in [33]. According to [33] the following estimates hold*

$$\|x(t_n) - x_n\| + \sum_{i=1}^k \|v_i(t_n) - v_{i,n}\| \leq Q\tau, \quad 1 \leq n \leq N,$$

which, together with (3.1), leads the following estimate between numerical solutions of different schemes

$$\begin{aligned} &\|x_n - X_n\| + \sum_{i=1}^k \|v_{i,n} - V_{i,n}\| \\ &\leq \|x(t_n) - x_n\| + \|x(t_n) - X_n\| \\ &\quad + \sum_{i=1}^k (\|v_i(t_n) - v_{i,n}\| + \|v_i(t_n) - V_{i,n}\|) \leq Q\tau. \end{aligned}$$

This implies that the difference between the numerical solutions turns to zero as τ decreases such that both methods generate almost the same numerical solutions for τ small enough. Nevertheless, the dynamics of directional vectors in (1.3) saves $O(d^2 N k^2)$ (or $O(d N k^2)$ if the dimer method [14] could be used to approximate the product of the Hessian matrix and the vector) computational cost in comparison with the scheme (1.5) that significantly improves the computational efficiency for large N , d or k .

3.2. Numerical experiments We carry out numerical experiments to test the convergence rate (denoted by ‘‘CR’’ in tables) of the numerical scheme (1.3) and compare the behavior between (1.3) and the scheme in [33]. We consider the following two-dimensional system proposed in [6]

$$E(x, y) = -\frac{1}{4}(x^2 - 1)^2 - \frac{1}{2}y^2. \quad (3.2)$$

For this system (0,0) is an index-1 saddle point and (1,0) is an index-2 saddle point.

Example 1: Accuracy test We compute the index-1 saddle point of (3.2) with the initial conditions

$$x_0 = \begin{bmatrix} 1 \\ 0.5 \end{bmatrix}, \quad v_{1,0} = \frac{1}{\sqrt{2}} \begin{bmatrix} -1 \\ -1 \end{bmatrix}$$

and the index-2 saddle point with the initial conditions

$$x_0 = \begin{bmatrix} 1.3 \\ 0.5 \end{bmatrix}, \quad v_{1,0} = \frac{1}{\sqrt{2}} \begin{bmatrix} -1 \\ -1 \end{bmatrix}, \quad v_{2,0} = \frac{1}{\sqrt{5}} \begin{bmatrix} -2 \\ -1 \end{bmatrix}.$$

As the exact solutions to the high-index saddle dynamics are not available, numerical solutions computed under $\tau = 2^{-13}$ serve as the reference solutions. We set $\beta = \gamma = 1$ and $T = 7$ to ensure that the saddle dynamics reaches the target saddle point. Numerical results are presented in Tables 3.1-3.2, which demonstrate the first-order accuracy of the numerical scheme (1.3) as proved in Theorem 3.1.

TABLE 3.1. Convergence rates of computing index-1 saddle point.

τ	$\max_n \ x(t_n) - x_n\ $	CR	$\max_n \ v_1(t_n) - v_{1,n}\ $	CR
2^{-6}	1.23E-01		9.83E-02	
2^{-7}	6.00E-02	1.04	4.94E-02	0.99
2^{-8}	2.92E-02	1.04	2.44E-02	1.02
2^{-9}	1.40E-02	1.06	1.18E-02	1.05

TABLE 3.2. Convergence rates of computing index-2 saddle point.

τ	$\max_n \ x(t_n) - x_n\ $	CR	$\max_n \ v_1(t_n) - v_{1,n}\ $	CR	$\max_n \ v_2(t_n) - v_{2,n}\ $	CR
2^{-6}	2.27E-01		1.43E-01		1.43E-01	
2^{-7}	1.09E-01	1.06	7.08E-02	1.01	7.08E-02	1.01
2^{-8}	5.28E-02	1.05	3.53E-02	1.00	3.53E-02	1.00
2^{-9}	2.53E-02	1.06	1.72E-02	1.03	1.72E-02	1.03

Example 2: Comparison between two schemes We compare the behavior between the scheme (1.3) and the scheme in [33] by selecting the same initial values and parameters as in the previous example and computing x_n and X_n in Figure 3.1,

which shows that both methods converge to the target saddle points along the same trajectory.

To compare the dynamical behavior of these two methods in a pointwise-in-time manner, we plot $\|x_n - X_n\|$ and $\|v_{1,n} - V_{1,n}\|$ in the computation of the index-1 saddle point under different time-step size τ in Figure 3.2, which shows that the differences between the numerical solutions of these two methods are quite small at each time step, and such differences shrink as τ decreases. In particular, it seems from Figure 3.2 that if τ becomes $\tau/2$, then the magnitudes of $\|x_n - X_n\|$ and $\|v_{1,n} - V_{1,n}\|$ also reduce by a half, which is consistent with the discussions in Remark 3.1.

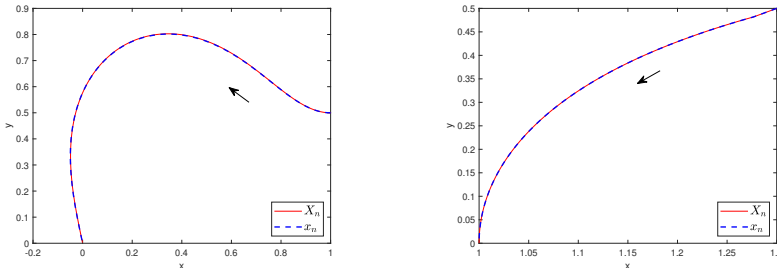


FIG. 3.1. Convergence of numerical solutions x_n and X_n to (left) the index-1 saddle point and (right) the index-2 saddle point under $T=7$ and $\tau=1/100$.

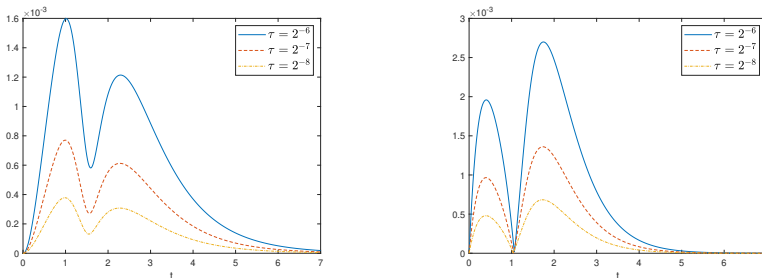


FIG. 3.2. Plots of (left) $\|x_n - X_n\|$ and (right) $\|v_{1,n} - V_{1,n}\|$ under $T=7$ and different τ when computing the index-1 saddle point.

4. Extension to constrained HiSD In this section we extend the developed methods and results for the constrained HiSD (1.6) to substantiate the conclusions in (ii) in Section 1.2.

4.1. Numerical discretization From the derivation of (1.6) in [23], the non-linear terms

$$-xx^\top F(x) \text{ and } \mathcal{L}_i - xx^\top J(x)v_i + xv_i^\top F(x) \quad (4.1)$$

in the equations of x and v_i are proposed to ensure the following manifold properties: if the following relations

$$x \in S^{d-1}, \quad v_i^\top x = 0, \quad v_i^\top v_j = \delta_{ij}, \quad 1 \leq i, j \leq k \quad (4.2)$$

hold at $t=0$, then they hold for any $t \geq 0$. In practical computations, the following efficient numerical scheme of (1.6) was proposed in [23] for $1 \leq n \leq N$

$$\begin{cases} \tilde{x}_n = x_{n-1} + \tau \mathcal{S}^{n-1}, \\ x_n = \frac{\tilde{x}_n}{\|\tilde{x}_n\|}, \\ \tilde{v}_{i,n} = v_{i,n-1} + \tau \mathcal{R}_i^{n-1}, \\ \hat{v}_{i,n} = \tilde{v}_{i,n} - \tilde{v}_{i,n}^\top x_n x_n, \\ v_{i,n} = \text{GramSchmidt}(v_{1,n}, \dots, v_{i-1,n}; \hat{v}_{i,n}), \quad 1 \leq i \leq k, \end{cases} \quad (4.3)$$

equipped with the initial state $x_0 \in S^{d-1}$ and orthonormal initial directional vectors $\{v_{i,0}\}_{i=1}^k$ such that $v_{i,0}^\top x_0 = 0$ for $1 \leq i \leq k$. Here the second equation of (4.3) represents the retraction in order to ensure that $x_n \in S^{d-1}$. The last two equations, which stand for the vector transport and the Gram-Schmidt orthonormalization procedure, respectively, aim to ensure the discrete analogue of (4.2), that is,

$$v_{i,n}^\top x_n = 0, \quad v_{i,n}^\top v_{j,n} = \delta_{ij}, \quad 1 \leq i, j \leq k, \quad 0 \leq n \leq N. \quad (4.4)$$

Furthermore, we use the explicit expression of the Gram-Schmidt orthonormalization as (2.1) with $\tilde{v}_{i,n}$ and $Y_{i,n}$ in (2.1) replaced by $\hat{v}_{i,n}$ and $Z_{i,n}$, respectively, for distinction.

4.2. Recovery of constrained HiSD The main result of this section is to recover the schemes of x and $\{v_i\}_{i=1}^k$ in the following theorem.

THEOREM 4.1. *For τ small enough, the following relations could be derived from the scheme (4.3)*

$$\begin{cases} \frac{x_n - x_{n-1}}{\tau} = \mathcal{S}^{n-1} - x_{n-1} x_{n-1}^\top F(x_{n-1}) + O(\tau), \\ \frac{v_{i,n} - v_{i,n-1}}{\tau} = \mathcal{R}_i^{n-1} + \mathcal{L}_i^{n-1} - x_{n-1} x_{n-1}^\top J(x_{n-1}) v_{i,n-1} \\ \quad + x_{n-1} v_{i,n-1}^\top F(x_{n-1}) + O(\tau), \quad 1 \leq i \leq k. \end{cases} \quad (4.5)$$

REMARK 4.1. *Similar to Remark 2.1, the recovered schemes in (4.5) have exactly the same forms as the continuous problem (1.6) such that the statements in (ii) could be justified.*

Proof. We prove this theorem in the following three steps.

Step 1: Derivation of the first equation in (4.5)

From the first equation of (4.3) we apply $x_{n-1}^\top v_{j,n-1} = 0$ to obtain

$$\|\tilde{x}_n\|^2 = 1 + 2\tau x_{n-1}^\top F(x_{n-1}) + O(\tau^2). \quad (4.6)$$

Then we use this and the second equation of (4.3) to obtain

$$\begin{aligned} x_n &= \tilde{x}_n + \frac{1 - \|\tilde{x}_n\|^2}{\|\tilde{x}_n\|(1 + \|\tilde{x}_n\|)} \tilde{x}_n \\ &= \tilde{x}_n + \frac{-2\tau x_{n-1}^\top F(x_{n-1}) + O(\tau^2)}{\|\tilde{x}_n\|(1 + \|\tilde{x}_n\|)} \tilde{x}_n \\ &= \tilde{x}_n - \tau x_{n-1}^\top F(x_{n-1}) \tilde{x}_n \\ &\quad - 2\tau x_{n-1}^\top F(x_{n-1}) \left(\frac{1}{\|\tilde{x}_n\|(1 + \|\tilde{x}_n\|)} - \frac{1}{2} \right) \tilde{x}_n + O(\tau^2). \end{aligned}$$

Similar to the estimate (2.13), the third right-hand side term is an $O(\tau^2)$ term, while, based on the first equation of (4.3), the second right-hand side term could be rewritten as

$$-\tau x_{n-1}^\top F(x_{n-1}) \tilde{x}_n = -\tau x_{n-1}^\top F(x_{n-1}) x_{n-1} + O(\tau^2).$$

We incorporate the above equations to get

$$x_n = \tilde{x}_n - \tau x_{n-1}^\top F(x_{n-1}) x_{n-1} + O(\tau^2),$$

which proves the first equation of (4.5).

Step 2: A preliminary estimate of $v_{i,n} - v_{i,n-1}$

The derivation of the second equation of (4.5) is much more complicated as we need to combine the last three equations in (4.3) by an appropriate manner. We first invoke the third equation of (4.3) in the fourth equation to obtain

$$\hat{v}_{i,n} = v_{i,n-1} + \tau J(x_{n-1}) v_{i,n-1} - (v_{i,n-1} + \tau J(x_{n-1}) v_{i,n-1})^\top x_n x_n.$$

From the first equation of (4.5) we have

$$v_{i,n-1}^\top x_n = -\tau v_{i,n-1}^\top F(x_{n-1}) + O(\tau^2).$$

Combining the above two equations and applying the substitution $x_n = x_{n-1} + O(\tau)$ (cf. the first equation of (4.5)) lead to

$$\begin{aligned} \hat{v}_{i,n} &= v_{i,n-1} + \tau J(x_{n-1}) v_{i,n-1} + \tau v_{i,n-1}^\top F(x_{n-1}) x_n \\ &\quad - \tau v_{i,n-1}^\top J(x_{n-1})^\top x_n x_n + O(\tau^2) \\ &= v_{i,n-1} + \tau J(x_{n-1}) v_{i,n-1} + \tau v_{i,n-1}^\top F(x_{n-1}) x_{n-1} \\ &\quad - \tau v_{i,n-1}^\top J(x_{n-1})^\top x_{n-1} x_{n-1} + O(\tau^2) \\ &=: v_{i,n-1} + \mathcal{L}_{i,n-1} + O(\tau^2), \\ \mathcal{L}_{i,n-1} &:= \tau J(x_{n-1}) v_{i,n-1} + \tau v_{i,n-1}^\top F(x_{n-1}) x_{n-1} \\ &\quad - \tau v_{i,n-1}^\top J(x_{n-1})^\top x_{n-1} x_{n-1}. \end{aligned} \tag{4.7}$$

We invoke this equation in the last equation of (4.3) to obtain

$$\begin{aligned} v_{i,n} &= \frac{1}{Z_{i,n}} \left(v_{i,n-1} + \mathcal{L}_{i,n-1} + O(\tau^2) \right. \\ &\quad \left. - \sum_{j=1}^{i-1} v_{j,n}^\top (v_{i,n-1} + \mathcal{L}_{i,n-1} + O(\tau^2)) v_{j,n} \right) \\ &= \frac{1}{Z_{i,n}} \left(v_{i,n-1} - \sum_{j=1}^{i-1} (v_{j,n} - v_{j,n-1})^\top v_{i,n-1} v_{j,n} + O(\tau) \right), \end{aligned} \tag{4.8}$$

which implies

$$\begin{aligned} v_{i,n} - v_{i,n-1} &= \frac{1}{Z_{i,n}} \left(v_{i,n-1} (1 - Z_{i,n}) - \sum_{j=1}^{i-1} (v_{j,n} - v_{j,n-1})^\top v_{i,n-1} v_{j,n} + O(\tau) \right). \end{aligned} \tag{4.9}$$

We also employ (4.7) to expand $Z_{i,n}$ as

$$\begin{aligned}
Z_{i,n} &= \left(1 + 2\tau v_{i,n-1}^\top J(x_{n-1}) v_{i,n-1} - \sum_{j=1}^{i-1} (v_{j,n}^\top v_{i,n-1})^2 + O(\tau^2) \right)^{1/2} \\
&= \left(1 + 2\tau v_{i,n-1}^\top J(x_{n-1}) v_{i,n-1} \right. \\
&\quad \left. - \sum_{j=1}^{i-1} ((v_{j,n} - v_{j,n-1})^\top v_{i,n-1})^2 + O(\tau^2) \right)^{1/2} \\
&= \left(1 - \sum_{j=1}^{i-1} ((v_{j,n} - v_{j,n-1})^\top v_{i,n-1})^2 + O(\tau) \right)^{1/2}.
\end{aligned} \tag{4.10}$$

Based on these equations we could follow the proof of Lemma 2.1 to prove that

$$\|v_{i,n} - v_{i,n-1}\| \leq Q\tau, \quad 1 \leq i \leq k, \quad 1 \leq n \leq N. \tag{4.11}$$

Step 3: Derivation of the second equation in (4.5) We invoke the estimate (4.11) back to the second equality of (4.10) to get

$$Z_{i,n} = (1 + 2\tau v_{i,n-1}^\top J(x_{n-1}) v_{i,n-1} + O(\tau^2))^{1/2}, \tag{4.12}$$

which, together with (2.12) and (2.13), implies

$$\frac{1}{Z_{i,n}} = 1 - \tau v_{i,n-1}^\top J(x_{n-1}) v_{i,n-1} + O(\tau^2).$$

We replace $1/Z_{i,n}$ in the first equality of (4.8) by this equation to get

$$\begin{aligned}
v_{i,n} &= v_{i,n-1} + \mathcal{L}_{i,n-1} - \sum_{j=1}^{i-1} v_{j,n}^\top (v_{i,n-1} + \mathcal{L}_{i,n-1}) v_{j,n} \\
&\quad - \tau v_{i,n-1}^\top J(x_{n-1}) v_{i,n-1} v_{i,n-1} \\
&\quad + \tau \sum_{j=1}^{i-1} v_{j,n}^\top v_{i,n-1} (v_{i,n-1}^\top J(x_{n-1}) v_{i,n-1}) v_{j,n} + O(\tau^2).
\end{aligned} \tag{4.13}$$

By (4.11), the last-but-one right-hand side term of (4.13) could be estimated as

$$\begin{aligned}
&\tau \sum_{j=1}^{i-1} v_{j,n}^\top v_{i,n-1} (v_{i,n-1}^\top J(x_{n-1}) v_{i,n-1}) v_{j,n} \\
&= \tau \sum_{j=1}^{i-1} (v_{j,n} - v_{j,n-1})^\top v_{i,n-1} (v_{i,n-1}^\top J(x_{n-1}) v_{i,n-1}) v_{j,n} \\
&= O(\tau^2),
\end{aligned}$$

and we reformulate the first summation on the right-hand side of (4.13) as

$$\begin{aligned}
& - \sum_{j=1}^{i-1} v_{j,n}^\top (v_{i,n-1} + \mathcal{L}_{i,n-1}) v_{j,n} \\
&= - \sum_{j=1}^{i-1} (v_{j,n} - \hat{v}_{j,n})^\top v_{i,n-1} v_{j,n} - \sum_{j=1}^{i-1} \hat{v}_{j,n}^\top v_{i,n-1} v_{j,n} \\
& \quad - \sum_{j=1}^{i-1} (v_{j,n} - v_{j,n-1})^\top \mathcal{L}_{i,n-1} v_{j,n} - \sum_{j=1}^{i-1} v_{j,n-1}^\top \mathcal{L}_{i,n-1} v_{j,n} \\
&=: \sum_{l=1}^4 B_l.
\end{aligned} \tag{4.14}$$

To bound B_1 , we apply the last equation of (4.3) to get

$$v_{j,n} - \hat{v}_{j,n} = \frac{1 - Z_{j,n}}{Z_{j,n}} \hat{v}_{j,n} - \frac{1}{Z_{j,n}} \sum_{l=1}^{j-1} \hat{v}_{j,n}^\top v_{l,n} v_{l,n},$$

which implies

$$(v_{j,n} - \hat{v}_{j,n})^\top v_{i,n-1} = \frac{1 - Z_{j,n}}{Z_{j,n}} \hat{v}_{j,n}^\top v_{i,n-1} - \frac{1}{Z_{j,n}} \sum_{l=1}^{j-1} \hat{v}_{j,n}^\top v_{l,n} v_{l,n}^\top v_{i,n-1}. \tag{4.15}$$

From (4.12) we find that $1 - Z_{j,n}$ is an $O(\tau)$ term, and $\hat{v}_{j,n}^\top v_{i,n-1}$ could be expanded as

$$\begin{aligned}
\hat{v}_{j,n}^\top v_{i,n-1} &= (\tilde{v}_{j,n} - \tilde{v}_{j,n}^\top x_n x_n)^\top v_{i,n-1} \\
&= (v_{j,n-1} + \tau J(x_{n-1}) v_{j,n-1})^\top v_{i,n-1} \\
& \quad - \tilde{v}_{j,n}^\top x_n x_n^\top (v_{i,n-1} - v_{i,n}) \\
&= (\tau J(x_{n-1}) v_{j,n-1})^\top v_{i,n-1} \\
& \quad - \tilde{v}_{j,n}^\top x_n x_n^\top (v_{i,n-1} - v_{i,n}) = O(\tau).
\end{aligned} \tag{4.16}$$

Thus the first right-hand side term of (4.15) is $O(\tau^2)$. The second right-hand side term of (4.15) could be reformulated as

$$\begin{aligned}
& - \frac{1}{Z_{j,n}} \sum_{l=1}^{j-1} \hat{v}_{j,n}^\top v_{l,n} v_{l,n}^\top v_{i,n-1} \\
&= - \frac{1}{Z_{j,n}} \sum_{l=1}^{j-1} \hat{v}_{j,n}^\top (v_{l,n} - v_{l,n-1}) v_{l,n}^\top (v_{i,n-1} - v_{i,n}) \\
& \quad - \frac{1}{Z_{j,n}} \sum_{l=1}^{j-1} \hat{v}_{j,n}^\top v_{l,n-1} v_{l,n}^\top (v_{i,n-1} - v_{i,n}).
\end{aligned} \tag{4.17}$$

By (4.11) the first right-hand side term of this equation is an $O(\tau^2)$ term, while, by a similar derivation as (4.16), the factor $\hat{v}_{j,n}^\top v_{l,n-1}$ in the second right-hand side term of this equation is an $O(\tau)$ term, which implies that the second right-hand side term of (4.17) and thus (4.15) are $O(\tau^2)$. Consequently, B_1 in (4.14) is $O(\tau^2)$.

To estimate B_2 , we find that

$$\begin{aligned}\tilde{v}_{j,n}^\top x_n &= (v_{j,n-1} + \tau J(x_{n-1})v_{j,n-1})^\top x_n \\ &= (v_{j,n-1} - v_{j,n})^\top x_n + \tau (J(x_{n-1})v_{j,n-1})^\top x_n = O(\tau),\end{aligned}$$

which, together with the third inequality of (4.16), implies

$$\hat{v}_{j,n}^\top v_{i,n-1} = (\tau J(x_{n-1})v_{j,n-1})^\top v_{i,n-1} + O(\tau^2).$$

Thus we could rewrite B_2 as

$$\begin{aligned}B_2 &= - \sum_{j=1}^{i-1} (\tau J(x_{n-1})v_{j,n-1})^\top v_{i,n-1} v_{j,n} + O(\tau^2) \\ &= - \sum_{j=1}^{i-1} (\tau J(x_{n-1})v_{j,n-1})^\top v_{i,n-1} v_{j,n-1} \\ &\quad - \sum_{j=1}^{i-1} (\tau J(x_{n-1})v_{j,n-1})^\top v_{i,n-1} (v_{j,n} - v_{j,n-1}) + O(\tau^2) \\ &= - \sum_{j=1}^{i-1} (\tau J(x_{n-1})v_{j,n-1})^\top v_{i,n-1} v_{j,n-1} + O(\tau^2).\end{aligned}$$

B_3 is clearly an $O(\tau^2)$ term, and we expand B_4 as

$$\begin{aligned}B_4 &= - \sum_{j=1}^{i-1} v_{j,n-1}^\top (\tau J(x_{n-1})v_{i,n-1} + \tau v_{i,n-1}^\top F(x_{n-1})x_{n-1} \\ &\quad - \tau v_{i,n-1}^\top J(x_{n-1})^\top x_{n-1} x_{n-1}) v_{j,n} \\ &= - \sum_{j=1}^{i-1} v_{j,n-1}^\top \tau J(x_{n-1})v_{i,n-1} v_{j,n} \\ &= - \sum_{j=1}^{i-1} v_{j,n-1}^\top \tau J(x_{n-1})v_{i,n-1} v_{j,n-1} \\ &\quad - \sum_{j=1}^{i-1} v_{j,n-1}^\top \tau J(x_{n-1})v_{i,n-1} (v_{j,n} - v_{j,n-1}) \\ &= - \sum_{j=1}^{i-1} v_{j,n-1}^\top \tau J(x_{n-1})v_{i,n-1} v_{j,n-1} + O(\tau^2).\end{aligned}$$

Invoking the estimates of $B_1 - B_4$ in (4.14) leads to

$$- \sum_{j=1}^{i-1} v_{j,n}^\top (v_{i,n-1} + \mathcal{L}_{i,n-1}) v_{j,n} = -2\tau \sum_{j=1}^{i-1} v_{j,n-1}^\top J(x_{n-1})v_{i,n-1} v_{j,n-1} + O(\tau^2),$$

and we incorporate this equation with (4.13) to obtain the second equation of (4.5), which completes the proof. \square

Based on this theorem, the error equations could be generated by subtracting the reference equations of (1.6) from (4.5), which, together with the conventional numerical

analysis method for systems of differential equations, lead to the following error estimate of the numerical scheme (4.3).

THEOREM 4.2. *Under the Assumption A, the following estimate holds for the numerical scheme (4.3) for τ sufficiently small*

$$\|x_n - x(t_n)\| + \sum_{i=1}^k \|v_{i,n} - v_i(t_n)\| \leq Q\tau, \quad 1 \leq n \leq N.$$

Here Q is independent from τ , n and N .

5. Concluding remarks In this paper we analyze an efficient discrete HiSD scheme, which drop the Lagrangian multiplier terms in HiSD and instead perform an additional Gram-Schmidt orthonormalization to ensure the Stiefel manifold constraint. We recover the same form as HiSD from this scheme, which not only generates error estimates naturally, but indicates that the mechanism of Stiefel manifold preservation in HiSD is nearly a Gram-Schmidt process. The developed methods are further extended to analyze the more complicated constrained HiSD on high-dimensional sphere, which reveal that the mechanisms of the constrained HiSD on preserving several manifold properties are close to simple operations such as the vector normalization, the vector transport and the Gram-Schmidt orthonormalization. These results reveal mechanisms of the HiSD and constrained HiSD in preserving several manifold properties via numerical analysis.

There are several other potential extensions of the current work that deserve further exploration. For instance, one could apply the projection method proposed in [11, Example 4.6] instead of the Gram-Schmidt process in (1.3) and (4.3) to retract the directional vectors back to the Stiefel manifold, which preserves the manifold property via the minimal adjustment. Specifically, let $\tilde{V}_n := [\tilde{v}_{n,1}, \dots, \tilde{v}_{n,k}] \in \mathbb{R}^{n \times k}$, then the projection $V_n := [v_{n,1}, \dots, v_{n,k}]$ could be determined by minimizing the Frobenius norm of the difference $\tilde{V}_n - V_n$ within the Stiefel manifold, i.e.

$$\min \|\tilde{V}_n - V_n\|_F \quad \text{subject to } V_n^\top V_n = I. \quad (5.1)$$

In practice, one could compute the singular value decomposition $\tilde{V}_n = U^\top \Sigma W$ and then the solution to (5.1) is $V_n = U^\top W$. Thus it is natural to consider to what extent the application of the projection method deviates the dynamics of the HiSD, or the possibility of designing a new form of HiSD whose mechanism of preserving the Stiefel manifold is nearly the projection method. As the solution of (5.1) does not have a clear form as the Gram-Schmidt process, more investigations are required to analyze these questions.

Furthermore, the ideas and techniques could be employed and improved to perform numerical analysis for HiSD constrained by m equalities [23, Equation 24]

$$\begin{cases} \frac{dx}{dt} = \mathcal{S}(t), \\ \frac{dv_i}{dt} = \left(I - v_i v_i^\top - 2 \sum_{j=1}^{i-1} v_j v_j^\top \right) \mathcal{H}(x)[v_i] \\ \quad - A(x) (A(x)^\top A(x))^{-1} \left(\nabla^2 c(x) \frac{dx}{dt} \right)^\top v_i, \quad 1 \leq i \leq k. \end{cases} \quad (5.2)$$

Here $c(x) = (c_1(x), \dots, c_m(x)) = 0$ represents the m equality constraints and $A(x) = (\nabla c_1(x), \dots, \nabla c_m(x))$. The constrained HiSD (1.6) is a special case of (5.2) with one

equality constraint

$$c_1(x) = \|x\|^2 - 1 = 0.$$

In this generalized constrained HiSD (5.2), $\mathcal{H}(x)$ refers to the Riemannian Hessian [23], which is difficult to compute and approximate in practice. Furthermore, compared with (1.6), additional complicated terms appear on the right-hand side of (5.2). These bring additional difficulties for the numerical analysis that we will investigate in the near future.

Acknowledgements. This work was partially supported by the National Natural Science Foundation of China (No. 12288101, 12225102, T2321001, 12301555), the Taisihan Scholars Program of Shandong Province (No. tsqn202306083), the National Key R&D Program of China (No. 2023YFA1008903).

REFERENCES

- [1] F. Bao, Y. Cao, A. Meir, W. Zhao, A first order scheme for backward doubly stochastic differential equations. *SIAM/ASA J. Uncertain. Quantif.* 4 (2016), 413–445. [3.1](#)
- [2] W. Bao, Y. Cai, Mathematical theory and numerical methods for Bose-Einstein condensation. *Kinetic and Related Models* 6 (2013), 1–135. [1.2](#)
- [3] W. Bao, Q. Du, Y. Zhang, Dynamics of rotating Bose-Einstein condensates and its efficient and accurate numerical computation. *SIAM J. Appl. Math.* 66 (2006), 758–786. [1.2](#)
- [4] J. Doye and D. Wales, Saddle points and dynamics of Lennard-Jones clusters, solids, and supercooled liquids. *J. Chem. Phys.* 116 (2002), 3777–3788. [1](#)
- [5] W. E, E. Vanden-Eijnden, Transition-path theory and path-finding algorithms for the study of rare events, *Annu. Rev. Phys. Chem.*, 61 (2010), 391–420. [1](#)
- [6] W. E and X. Zhou, The gentlest ascent dynamics. *Nonlinearity* 24 (2011), 1831–1842. [1](#), [3.2](#)
- [7] P. E. Farrell, Å. Birkisson, and S. W. Funke, Deflation Techniques for Finding Distinct Solutions of Nonlinear Partial Differential Equations. *SIAM J. Sci. Comput.* 37 (2015), A2026–A2045. [1](#)
- [8] W. Gao, J. Leng, and X. Zhou, An iterative minimization formulation for saddle point search. *SIAM J. Numer. Anal.* 53 (2015), 1786–1805. [1](#)
- [9] N. Gould, C. Ortner and D. Packwood, A dimer-type saddle search algorithm with preconditioning and linesearch. *Math. Comp.* 85 (2016), 2939–2966. [1](#)
- [10] W. Grantham, Gradient transformation trajectory following algorithms for determining stationary min-max saddle points, in *Advances in Dynamic Game Theory*, Ann. Internat. Soc. Dynam. Games 9, Birkhauser Boston, Boston, MA, 2007, 639–657. [1](#)
- [11] E. Hairer, C. Lubich, G. Wanner, Geometric numerical integration: Structure-preserving algorithms for ordinary differential equations, 2nd edn., Springer, Berlin, 2006. [1.1](#), [5](#)
- [12] Y. Han, Y. Hu, P. Zhang, A. Majumdar, L. Zhang, Transition pathways between defect patterns in confined nematic liquid crystals. *J. Comput. Phys.* 396 (2019), 1–11. [1](#)
- [13] Y. Han, J. Yin, Y. Hu, A. Majumdar, L. Zhang, Solution landscapes of the simplified Ericksen-Leslie model and its comparison with the reduced Landau-de Gennes model, *Proceedings of the Royal Society A*, 477 (2021), 20210458. [1](#)
- [14] G. Henkelman, H. Jónsson, A dimer method for finding saddle points on high dimensional potential surfaces using only first derivatives. *J. Chem. Phys.* 111 (1999), 7010–7022. [3.1](#)
- [15] A. Levitt and C. Ortner, Convergence and cycling in walker-type saddle search algorithms. *SIAM J. Numer. Anal.* 55 (2017), 2204–2227. [1](#)
- [16] Y. Li and J. Zhou, A minimax method for finding multiple critical points and its applications to semilinear PDEs, *SIAM J. Sci. Comput.* 23 (2001), 840–865. [1](#)
- [17] Z. Li, J. Zhou, A local minimax method using virtual geometric objects: Part II—For finding equality constrained saddles. *J. Sci. Comput.* 78 (2019), 226–245. [1](#)
- [18] W. Liu, Z. Xie, W. Yi, Normalized Wolfe-Powell-type local minimax method for finding multiple unstable solutions of nonlinear elliptic PDEs. *Sci. China Math.* 66 (2023), 2361–2384. [1](#)
- [19] D. Mehta, Finding all the stationary points of a potential-energy landscape via numerical polynomial-homotopy-continuation method, *Phys. Rev. E* 84 (2011), 025702. [1](#)
- [20] J. W. Milnor, *Morse Theory*, Princeton University Press, 1963. [1](#)
- [21] W. Wang, L. Zhang, P. Zhang, Modelling and computation of liquid crystals. *Acta Numerica* 30 (2021), 765–851. [1](#)

- [22] Z. Xie, Y. Yuan, J. Zhou, On solving semilinear singularly perturbed Neumann problems for multiple solutions. *SIAM J. Sci. Comput.* 44 (2022), A501–A523. [1](#)
- [23] J. Yin, Z. Huang, L. Zhang, Constrained high-index saddle dynamics for the solution landscape with equality constraints, *J. Sci. Comput.* 91 (2022), 62. [1,2](#), [4,1](#), [4,1](#), [5](#), [5](#)
- [24] J. Yin, K. Jiang, A.-C. Shi, P. Zhang, L. Zhang, Transition pathways connecting crystals and quasicrystals, *Proc. Natl. Acad. Sci. U.S.A.*, 118 (2021), e2106230118. [1](#)
- [25] J. Yin, Y. Wang, J. Chen, P. Zhang, L. Zhang, Construction of a pathway map on a complicated energy landscape. *Phys. Rev. Lett.* 124 (2020), 090601. [1](#)
- [26] J. Yin, B. Yu, L. Zhang, Searching the solution landscape by generalized high-index saddle dynamics. *Sci. China Math.* 64 (2021), 1801. [1](#), [1,1](#), [1,1](#)
- [27] J. Yin, L. Zhang, P. Zhang, High-index optimization-based shrinking dimer method for finding high-index saddle points. *SIAM J. Sci. Comput.* 41 (2019), A3576–A3595. [1](#), [1](#), [1,1](#)
- [28] B. Yu, X. Zheng, P. Zhang, L. Zhang, Computing solution landscape of nonlinear space-fractional problems via fast approximation algorithm. *J. Comput. Phys.* 468 (2022), 111513. [1](#)
- [29] J. Zhang, Q. Du, Shrinking dimer dynamics and its applications to saddle point search. *SIAM J. Numer. Anal.* 50 (2012), 1899–1921. [1](#)
- [30] J. Zhang, Q. Du, Constrained shrinking dimer dynamics for saddle point search with constraints. *J. Comput. Phys.* 231 (2012), 4745–4758. [1,2](#)
- [31] L. Zhang, W. Ren, A. Samanta, Q. Du, Recent developments in computational modelling of nucleation in phase transformations. *npj Comput. Mater.* 2 (2016), 16003. [1](#)
- [32] L. Zhang, Q. Du, Z. Zheng, Optimization-based shrinking dimer method for finding transition states. *SIAM J. Sci. Comput.* 38 (2016), A528–A544. [1](#)
- [33] L. Zhang, P. Zhang, X. Zheng, Error estimates of Euler discretization to high-index saddle dynamics. *SIAM J. Numer. Anal.* 60 (2022), 2925–2944. [1,1](#), [1,1](#), [2](#), [3,1](#), [3,2](#), [3,2](#)
- [34] L. Zhang, P. Zhang, X. Zheng, Discretization and index-robust error analysis for constrained high-index saddle dynamics on the high-dimensional sphere. *Sci. China Math.* 66 (2023), 2347–2360.